© 2016. Published by The Company of Biologists Ltd | Journal of Cell Science (2016) 129, 492-501 doi:10.1242/jcs.173666

RESEARCH ARTICLE

Germline deletion of huntingtin causes male infertility and arrested spermiogenesis in mice

Jinting Yan[1], Hui Zhang[1], Yang Liu[1], Feilong Zhao[1], Shu Zhu[2], Chengmei Xie[1], Tie-Shan Tang[2,*] and Caixia Guo[1,*]

ABSTRACT

Human Huntingtin (*HTT*), a Huntington's disease gene, is highly expressed in the mammalian brain and testis. Simultaneous knockout of mouse Huntingtin (*Htt*) in brain and testis impairs male fertility, providing evidence for a link between *Htt* and spermatogenesis; however, the underlying mechanism remains unclear. To understand better the function of *Htt* in spermatogenesis, we restricted the genetic deletion specifically to the germ cells using the Cre/*loxP* site-specific recombination strategy and found that the resulting mice manifested smaller testes, azoospermia and complete male infertility. Meiotic chromosome spread experiments showed that the process of meiosis was normal in the absence of *Htt*. Notably, we found that *Htt*-deficient round spermatids did not progress beyond step 3 during the post-meiotic phase, when round spermatids differentiate into mature spermatozoa. Using an iTRAQ-based quantitative proteomic assay, we found that knockout of *Htt* significantly altered the testis protein profile. The differentially expressed proteins exhibited a remarkable enrichment for proteins involved in translation regulation and DNA packaging, suggesting that Htt might play a role in spermatogenesis by regulating translation and DNA packaging in the testis.

KEY WORDS: Huntingtin, Spermiogenesis, Translation, Spermatogenesis, DNA packaging

INTRODUCTION

The human Huntingtin gene (*HTT*) is a disease gene linked to Huntington's disease, a neurodegenerative disorder characterized by loss of striatal and cortical neurons (Gil and Rego, 2008). Given that expansion of a CAG triplet repeat encoding polyglutamine within the *HTT* gene causes Huntington's disease, most studies on mouse Huntingtin (*Htt*) have focused on elucidating the underlying mechanism(s) of how the mutant Htt (mHtt) leads to neurodegeneration. Little is known about the cellular function of wild-type (WT) Htt. The complete inactivation of Htt in mice causes embryonic death before day 8.5 (Nasir et al., 1995; Zeitlin et al., 1995; Dragatsis et al., 2000), indicating that Htt is essential for embryonic development (White et al., 1997; Auerbach et al., 2001). Notably, the human mutant HTT (mHTT) does not seem to abrogate the developmental functions of HTT, as Huntington's disease patients only start to manifest symptoms years after birth. Moreover, human mHTT can compensate for the absence of endogenous *Htt* gene, by rescuing the embryonic lethality of mice with a targeted disruption of both copies of the endogenous *Htt* gene (Leavitt et al., 2001).

[1]CAS Key Laboratory of Genomic and Precision Medicine, China Gastrointestinal Cancer Research Center, Beijing Institute of Genomics, Chinese Academy of Sciences, Beijing 100101, China. [2]State Key Laboratory of Membrane Biology, Institute of Zoology, Chinese Academy of Sciences, Beijing 100101, China.

*Authors for correspondence (guocx@big.ac.cn; tangtsh@ioz.ac.cn)

Received 29 April 2015; Accepted 7 December 2015

Htt is a large protein with unknown function that is expressed ubiquitously at low levels during early development and at high levels in the testis and in neurons of the brain (Van Raamsdonk et al., 2007). Within the cell, mammalian Htt is associated with a variety of organelles, including the nucleus, endoplasmic reticulum, Golgi complex and mitochondrion. This widespread subcellular localization indicates its various functions, including anti-apoptosis, facilitation of vesicular transport, control of brain-derived neurotrophic factor (BDNF) production, neuronal gene transcription and synaptic transmission (Cattaneo et al., 2005). The role of Htt in post-transcriptional regulation has been postulated to link to Huntington's disease pathogenesis. Htt localizes in P granules, which are centers of mRNA storage, degradation and small-RNA-mediated gene silencing. Consistently, Htt associates with argonaute 2 (Ago2, the catalytic component of the RNA-induced silencing complex) (Savas et al., 2008) and is also involved in RNA transport in cultured cortical neurons (Savas et al., 2010). Recently, both WT and mHtt have been found to co-purify with several translation-related proteins, and co-fractionate with ribosomes. Furthermore, Htt overexpression inhibits cap-dependent translation of a reporter mRNA in an *in vitro* system (Culver et al., 2012).

Interestingly, by employing the Cre/loxP site-specific recombination strategy to inactivate Htt expression in the mouse forebrain, but using a line that also deletes Htt in male germ cells, Ioannis Dragatsis et al. have found that the generated conditional knockout mice display reduced Htt expression in testis and severe spermatogenesis arrest. The mutant seminiferous tubules were disorganized and contained fewer spermatocytes and round spermatids compared with controls. They also observed a corresponding reduction in the number of mature motile sperm in the lumen of the mutant epididymis (Dragatsis et al., 2000). These results hint that Htt might play an essential role during spermatogenesis in testis. However, considering that the Camk2a-cre lines they employed can induce a simultaneous deletion of floxed *Htt* gene in the brain and male germ cells (Choi et al., 2014), it is necessary to generate a germ-cell-conditional knockout mouse (CKO) model to directly confirm the possibility.

Spermatogenesis is a major function of mammalian testis, covering the processes involved in production of spermatagonia to mature sperm. Spermatogenesis is characterized by three phases, mitosis, meiosis and spermiogenesis. During meiosis, spermatocytes pass through six different stages, distinguished by the morphology of the meiotic chromosomes. While in spermiogenesis, round spermatids pass through 16 stages to differentiate into spermatozoa, which have specialized organelles for motility and fertilization (Oakberg, 1956). During spermatogenesis, translational regulation plays an important role in the development of spermatocytes and spermatids (Paronetto and Sette, 2010; Nguyen-Chi and Morello, 2011; Idler and Yan, 2012; Kleene, 2013). Many mRNA transcribed in spermatocytes and

Journal of Cell Science

Journal of Cell Science (2016) 129, 492-501 doi:10.1242/jcs.173666

round spermatids are stored in a translationally inactive state for several days to more than two weeks, before their protein products can be detected in elongating and elongated spermatids. Additionally, translational control directs the onset and the end of the first meiotic phase, with most of the mRNAs in pachytene spermatocytes and round spermatids partially repressed by an unknown mechanism (Kleene, 2013).

In this report, we generated a conditional knockout mouse (CKO) with the promoter of *Stra8* to specifically promote the expression of Cre in the male germ cells. We show that the germline-specific ablation of *Htt* in mouse testes results in a male infertility, with a specific defect in spermiogenesis. In order to study the molecular mechanism of Htt in spermatogenesis, we employed a quantitative proteomic approach based on isobaric tags for relative and absolute quantification (iTRAQ) to investigate the differentially expressed proteins in testis in the absence of Htt. We found that knockout of *Htt* significantly altered the testis protein profile. The differentially expressed proteins were mainly enriched in the pathway involved in translation regulation and DNA packaging, suggesting that male infertility in *Htt* CKO mice could be partially attributed to the role of Htt in protein synthesis and chromatin remodeling.

RESULTS

Specific deletion of *Htt* in the male germ cells results in severe infertility and impairs spermatogenesis

To determine the role of Htt in spermatogenesis and male fertility, the Cre/loxP system was used to inactivate Htt in male germ cells. We generated a germ-cell-specific *Htt* CKO mice model by mating $Htt^{flox/flox}$ mice harboring two loxP sites inserted 1.3 kb upstream of the *Htt* transcription initiation site and within intron 1 with Stra8-cre mice (Fig. 1A) (Dragatsis et al., 2000). The *Stra8* promoter drives Cre expression in germ cells starting from primitive spermatogonia at postnatal day (P)5, and then, from P10 onwards, becomes prominent in preleptotene spermatocytes, and is not detected in other tissues examined (Vernet et al., 2006). When Stra8-cre transgenic males are bred with female mice containing a *Htt* floxed sequence, Cre-mediated recombination will result in deletion of the *Htt*, specifically during these stages of spermatogenesis. Given that loss of one allele of *Htt* in testes has no apparent effects on spermatogenesis and fertility, $Htt^{flox/flox}$ and $Htt^{\Delta/flox}$ were together used as controls. $Htt^{flox/flox}$/Stra8-cre mice and $Htt^{\Delta/flox}$/Stra8-cre mice were used as the CKO group (Fig. 1A).

To test the fertility of *Htt* deficient males, we mated CKO male mice with WT females and monitored the breeding capacity within 3 months of mating. The percentage of females plugged was similar between the controls and *Htt* CKO male mice, suggesting that inactivation of Htt expression in germ cells has no effect on mating capacity. However, no *Htt* CKO mice were able to father litters, whereas the average litter number for the control male mice was 8±1.4 (Table 1). Meanwhile, epididymal sperm counts of CKO animals yielded no detectable sperm, indicating that the CKO mice were azoospermic (Table 1).

To understand the underlying mechanism for the male infertility in *Htt*-deficient mice, we harvested the testes and performed histological staining. We found that depletion of *Htt* resulted in smaller testes in adult mice. The testis weights were significantly reduced in *Htt* CKO mice as early as postnatal week 6, suggesting that *Htt* deficiency might impair the first wave of spermatogenesis (Fig. 1B,C). The testes from *Htt* CKO mice display an obvious abnormality in histological analysis, with many tubules filling with large vacuolated spaces and lacking late-stage germ cells. Additionally, a more disordered arrangement of germ cells in

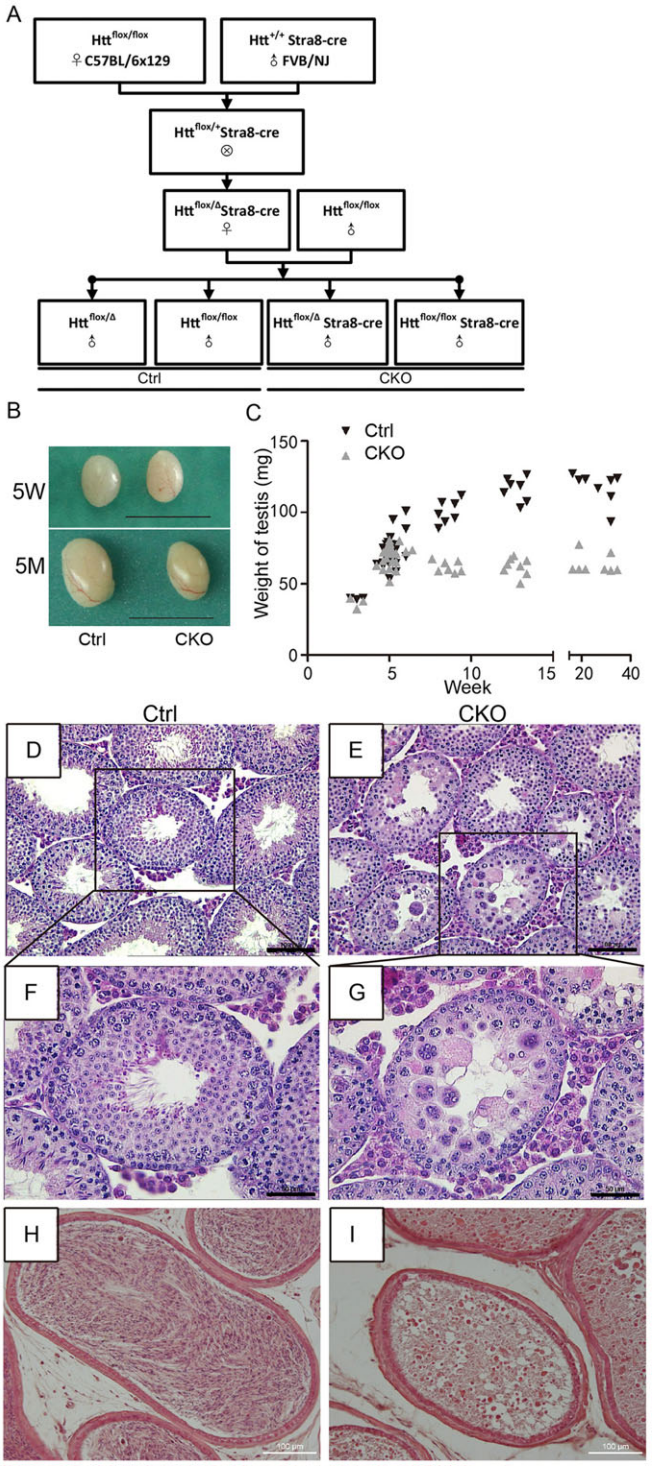

Fig. 1. The generation and phenotype of male *Htt* CKO mice. (A) The breeding scheme for the *Htt* CKO mice. $Htt^{flox/flox}$ mice were mated with Stra8-cre mice to generate mice as conditional knockout group (CKO) and control group (Ctrl). The genotypes of the last row were used as the Ctrl and CKO group in this study. The genetic background of the parental mouse strain is indicated within the block diagram. (B) Photographs of testes from 5-week- and 5-month-old *Htt* CKO and control mice from Stra8-cre and *Htt*-Flox crosses, respectively. (C) Weights of testes from control mice and CKO mice (3- to 32-week-old). (D,E) Histological analysis of seminiferous tubules in 6-week-old mice at low magnifications. (F,G) Histological analysis of seminiferous tubules in 6-week-old mice at high magnifications. (H,I) H&E-stained sections of epididymides from 8-week-old mice. Scale bars: 1 cm (B); 100 µm (D,E); 50 µm (F,G); 100 µm (H,I).

Journal of Cell Science (2016) 129, 492-501 doi:10.1242/jcs.173666

Table 1. Male fertility data from *Htt* CKO mice and control mice at 8 weeks of age

Genotype	*n*	Plugs	Fertility	Litter size[a]	Sperm count[b]	Sperm motility[b]
Control	3	100%	100%	8.0±1.4	$2.0\times10^7\pm1.2\times10^6$	Yes, moving well
CKO	3	100%	0%	0	No sperm	No sperm

[a]The mean of litter size from all the female mice (±s.d.).
[b]Count and motility of isolated sperm from epididymides was assessed under microscope. Sperm count is the mean of three mice per group (±s.d.).

seminiferous tubules was seen in *Htt* CKO mice, with scattered multinucleated germ cells and eosinophilic materials in the epithelial layer and lumen of CKO testes. In contrast, the testes from the control littermates contain germ cells of all developmental stages: spermatogonia, meiotic spermatocytes, postmeiotic round spermatids and elongating spermatids (Fig. 1D–G). Consistent with this, a Prm2 immunofluorescence assay revealed that the signal of Prm2 was significantly reduced in *Htt* CKO mice compared to the control mice (Fig. S1). Only degenerating spermatozoa were detected in *Htt* CKO epididymides when we examined the histology of the adult epididymides (Fig. 1H,I). Taken together, these data indicate that Htt is required for male fertility and spermatogenesis.

Loss of *Htt* does not impair the proliferation and differentiation of spermatogonia

Given that the number of germ cells within CKO seminiferous tubules was substantially reduced, we wondered whether this could be attributed to a reduction in the number of spermatogonia. Upon analyzing the staining of PLZF (also known as ZBTB16), whose expression is restricted to undifferentiated spermatogonia and which is required for stem cell self-renewal (Costoya et al., 2004), we could not detect any significant difference in the proportion of PLZF-positive spermatogonia between WT and CKO testes (Fig. 2A,B). In addition, both control and CKO tubules exhibited a basal layer of cells positive for PCNA (a mitotic proliferation marker), suggesting that mitotic proliferation is unaffected in CKO tubules (Fig. 2C,D). After mitosis, spermatogonia differentiate to enter into meiotic prophase, beginning as preleptotene spermatocytes. We wanted to know whether the onset of meiosis is affected in *Htt* CKO mice. Hence, we examined the expression of DAZL, which is expressed in the cytoplasm of spermatocytes (Lifschitz-Mercer et al., 2002) in CKO mice. We could not detect any abnormality in spermatocytes of 3-week-old CKO testes, indicating that spermatogonia can differentiate into meiotic spermatocytes in the absence of Htt (Fig. 2E,F).

Loss of *Htt* does not affect DNA double-strand break formation, homologous chromosome synapsis and crossover in meiosis

During meiosis, a large number of DNA double-strand breaks (DSBs) are produced. We thus monitored the signal of the phosphorylated form of histone variant H2AX (γH2AX), which is a well-defined DSB marker. As reported previously, γH2AX was expressed in all preleptotene to zygotene spermatocytes, whereas in pachytene spermatocyte γH2AX only presented in the sex vesicle (Hamer et al., 2003) (Fig. 3E). No substantial differences in γH2AX localization were detected in zygotene and pachytene spermatocytes from 3-week-old WT and *Htt* CKO mice (Fig. 3A,B). However, several seminiferous tubules contained more than one layer of zygotene or pachytene spermatocytes in 6-week-old *Htt* CKO mice (Fig. 3C–F).

To check whether Htt inactivation affects the key events of meiotic prophase, we performed meiotic chromosome spreads from WT and *Htt* CKO mice. No substantial differences in γH2AX localization in pachytene and diplotene spermatocytes could be observed (Fig. 4A). To determine whether deleting *Htt* in the CKO testis results in meiotic defects or spermatocyte depletion, we examined the dynamics of chromosome synapsis and recombination using antibodies directed against the synaptonemal complex proteins SYCP1 and SYCP3, which are components of the meiotic nodules and chromatin markers. During spermatogenesis, SYCP3 proteins begin to assemble along each sister-chromatid pair at leptonema to form the axial element, which represents the precursor of the synaptonemal complex and, subsequently, becomes a major component of the synaptonemal complex lateral elements during zygonema. SYCP1, which appears at zygonema, is a major component of the synaptonemal complex central element, and is used as a marker of fully synapsed chromosome segments. In control and CKO pachytene spermatocytes, SYCP1 and SYCP3 decorated the axes of all 19 completely synapsed autosomes. Based on the dynamic signaling of SYCP1 and SYCP3, no apparent

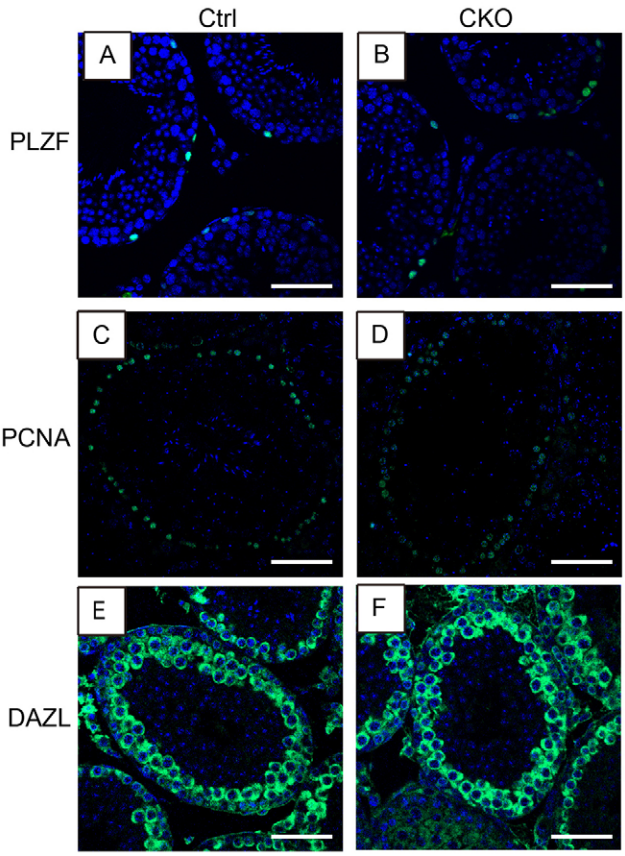

Fig. 2. Loss of *Htt* shows normal number and proliferation of spermatogonia. Sections from 8-week-old control (Ctrl) and CKO mouse testes were stained with the anti-Plzf (A,B), anti-PCNA (C,D) antibodies. Sections from 3-week-old control and CKO mouse testes were stained with the anti-DAZL antibody (E,F). Scale bars: 50 µm.

Journal of Cell Science (2016) 129, 492-501 doi:10.1242/jcs.173666

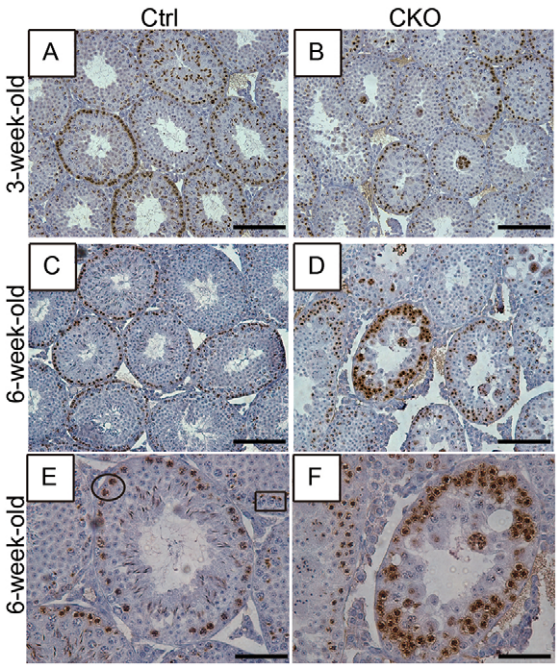

Fig. 3. Loss of *Htt* does not affect the production of DNA DSBs during meiosis. Sections from 3- and 6-week-old control (Ctrl) and CKO mouse testes were stained with the anti-γH2AX antibody. Pachytene spermatocytes were identified by the γH2AX-positive sex body (cells inside rectangle in E). Zygotene spermatocytes were marked by the strong γH2AX signaling over the whole nucleus (cells inside ellipse in E). Scale bars: 100 µm (A–D); 50 µm (E,F).

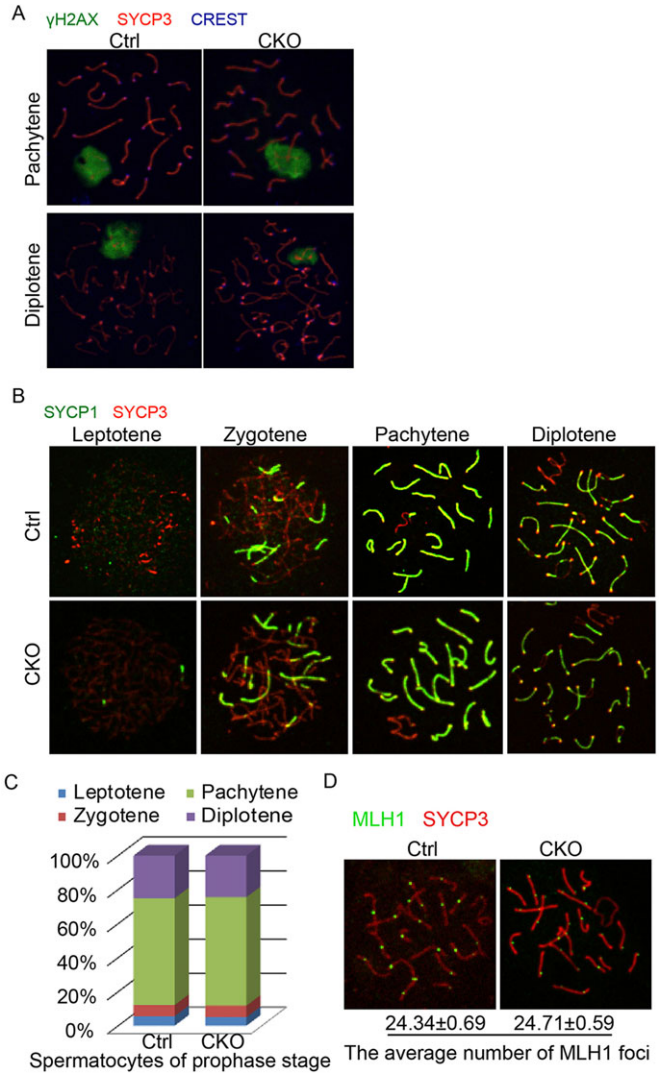

Fig. 4. Loss of *Htt* does not affect homologous chromosome synapsis and crossover in meiosis. Immunofluorescence staining was performed on spread chromosomes from 6-week-old male primary spermatocytes, and cells were imaged by laser confocal microscopy. (A) The γH2AX signal does not show appreciable differences between the control (Ctrl) and CKO testes. Testicular cells were spread and then stained with anti-γH2AX (green), anti-SYCP3 (red) and anti-Crest (blue) antibodies. SYCP3 accumulates on chromosomes beginning in leptotene and is present along their full length during pachytene. γH2AX accumulates from leptotene to zygotene and is restricted to the sex chromosomes at the pachytene and diplotene stages. (B) The assembly and disassembly of the synaptonemal complex is not affected by knockout of *Htt*. Testicular cells were spread and then stained with anti-SYCP1 (green) and anti-SYCP3 (red) antibodies. The developmental stages of meiotic prophase based on SYCP1 and SYCP3 kinetics are indicated in each panel. (C) The proportion of cells in each meiotic phase in the control and CKO testes (n=3). (D) Testicular cells were spread and then stained with anti-MLH1 (green) and anti-SYCP3 antibody (red). The mean±s.d. numbers of MLH1 foci per pachytene cell (n=3) are from three mice.

difference was seen in the formation and dissolution of the synaptonemal complex from *Htt* CKO mice compared with those of control mice (Fig. 4B). Meanwhile, we did not detect any significant change in the proportion of leptotene, zygotene, pachytene and diplotene between 6-week-old control and *Htt* CKO mice (Fig. 4C). These data suggest that Htt deficiency does not impair the formation and disassembly of the synaptonemal complex.

We further probed meiotic chromosomes with an antibody directed against the mismatch repair protein MLH1, a marker of chiasmata. We found that the mid-pachytene chromosomes from WT and CKO mice displayed one or two MLH1 foci per synapsed homologue. The average number of MLH1 foci in pachytene cells exhibited no significant difference between contol and CKO pachytene cells (Fig. 4D). Therefore, no defect in prophase I of meiosis could be detected in *Htt* CKO mice (indicated by the hollow arrow in Fig. 5I,J).

Spermiogenesis is interrupted at the Golgi phase upon Htt deficiency

Given that *Htt* CKO mice lack elongated spermatids in testis (Fig. 1D–I), we next examined whether spermiogenesis, during which round spermatids differentiate into mature spermatozoa, was affected by Htt deficiency. The process of spermiogenesis lasts about 13 days in mice and is divided into 16 developmental steps, which can be distinguished based on the morphology of the nucleus and acrosome, as well as associations between germ cells at different stages of spermatogenesis (Oakberg, 1956; Russell et al., 1990). It usually covers four phases: Golgi (steps 1–3), cap (steps 4–7), acrosomal (steps 8–12) and maturation (steps 13–16) (Oakberg, 1956). To pinpoint the exact arrest point in *Htt* CKO mice, we stained the puberal testis sections with the acrosome marker equatorin (EQTN, also known as AFAF) (Li et al., 2006). As shown in Fig. 5, the acrosome was detected as a purple-magenta signal on the nuclear envelope of round spermatids, as well as along one edge of the elongated spermatid head in the control mice (Fig. 5C,E,G and I). Intriguingly, in *Htt* CKO mice, round spermatids were present in stage I–VII tubules, but by stage II–III not all spermatids had the normal acrosome granules indicative of step 3 at the Golgi

Journal of Cell Science (2016) 129, 492-501 doi:10.1242/jcs.173666

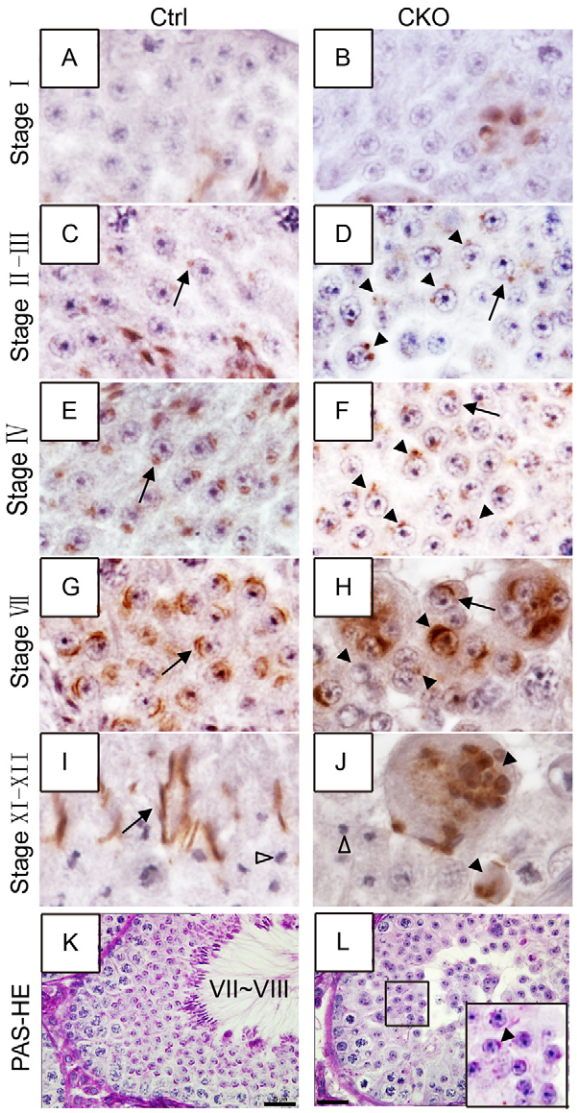

Fig. 5. Spermiogenesis is arrested at step 3 spermatid in CKO testes. (A–J) Immunohistochemistry for the acrosome marker AFAF in testis sections from 6-week-old mice. Representative control (Ctrl) and CKO sections showing stage I (A,B), stage II–III (C,D), stage IV (E,F), stage VII (G,H) and stage XI–XII (I,J) seminiferous tubules. Black arrows indicate spermatids with normal acrosomes. Black arrowheads indicate round spermatids with abnormal acrosomes (C–J). Unfilled arrowheads indicate metaphase spermatocytes (I,J). (K–L) PAS–hematoxylin-stained cross sections of seminiferous tubules from 6-week-old control and *Htt* CKO mice. The black arrowhead indicates a spermatid at about step 3 (L). Scale bars: 25 µm (K,L).

phase, and many had two pre-acrosomal vesicles that failed to fuse (indicated with arrowhead in Fig. 5D). Additionally, the acrosome of spermatids showed a range of malformations inside seminiferous tubules after stage III. Most spermatids had earlier step 2 acrosomes or two pre-acrosomal vesicles, only a few had developed to step 7, and none has progressed further than step 7 (indicated with arrowhead in Fig. 5F,H,J). We also observed that spermiogenesis was blocked at step 3 by performing periodic acid Schiff's staining (PAS) (Fig. 5K,L). These results indicate that most of the round spermatids do not develop beyond step 3 of spermiogenesis in *Htt* CKO mice.

As indicated above, multinucleated giant cells were present in *Htt* CKO testis, which is indicative of apoptosis (Nantel et al., 1996). We also examined whether depletion of Htt provokes germ cell apoptosis through TUNEL staining. We found the amount of apoptotic germ

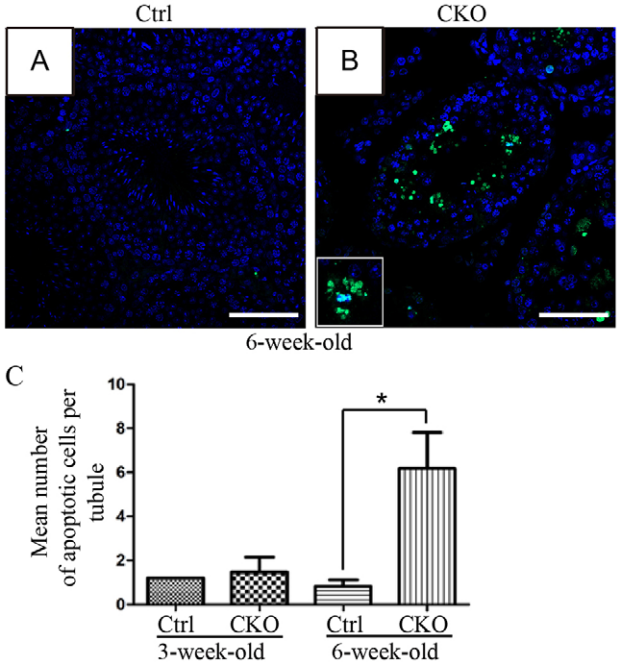

Fig. 6. TUNEL staining of testes sections from the control and *Htt* CKO mice. TUNEL staining images of testes sections from 6-week-old control (Ctrl) and CKO mice (A,B). Cells in the square frame in B indicate the characteristic multinucleated giant cells and cells with an abnormal nuclear structure. Most multinucleate round spermatids and some isolated round spermatid were apoptotic, whereas no increase in apoptosis was detected in other types of cells. (C) The number of TUNEL-positive cells per tubule cross section in control and *Htt* CKO mice aged 3 weeks or 6 weeks. There is a significant difference in the number of apoptotic cells per tubule between the control and Htt CKO mice at 6 weeks of age (n=3). *P<0.05 (unpaired t-test). Scale bar: 50 µm.

cells was similar between WT and *Htt* CKO mice at 3 weeks of age. Interestingly, *Htt* CKO testes manifest a significant increase in the amount of apoptotic germ cells compared to the controls at 6 weeks of age (Fig. 6), most abundantly at multinucleated round spermatids (Fig. 6B). These results suggest that germ cell development in the *Htt* CKO mice is impaired at the early round spermatid stage.

Differentially expressed protein identification through iTRAQ analysis

To elucidate the underlying mechanism of how Htt affects spermiogenesis, we compared the global protein expression profiles between the control and *Htt* KO testes from 5-week-old mice by using an iTRAQ-based quantitative proteomic approach. To ensure reliable identification, the following conditions were set to ensure reliable analysis: (1) a false discovery rate (FDR)<1%; and (2) only accepting proteins identified with at least one unique peptide. Our tandem mass spectrometry (MS/MS) analysis identified a total of 328,455 mass spectra. After data filtering to exclude low-scoring spectra, 74,233 unique spectra matched to special peptides were obtained. Searching using Mascot 2.3.0 identified a total of 20,598 peptides from 3481 proteins (Table S1). Considering that iTRAQ quantification usually underestimates the 'real' fold change between samples (Karp et al., 2010; Zhang et al., 2014), expression differences greater than 1.2-fold with a P<0.05 were applied to classify proteins of interest and potential significance for further investigations. Results showed that 119 proteins (42 upregulated and 77 downregulated) exhibited significant differential expression in Htt-deficient testes, which included the significantly downregulated Htt (Table S1).

Journal of Cell Science (2016) 129, 492-501 doi:10.1242/jcs.173666

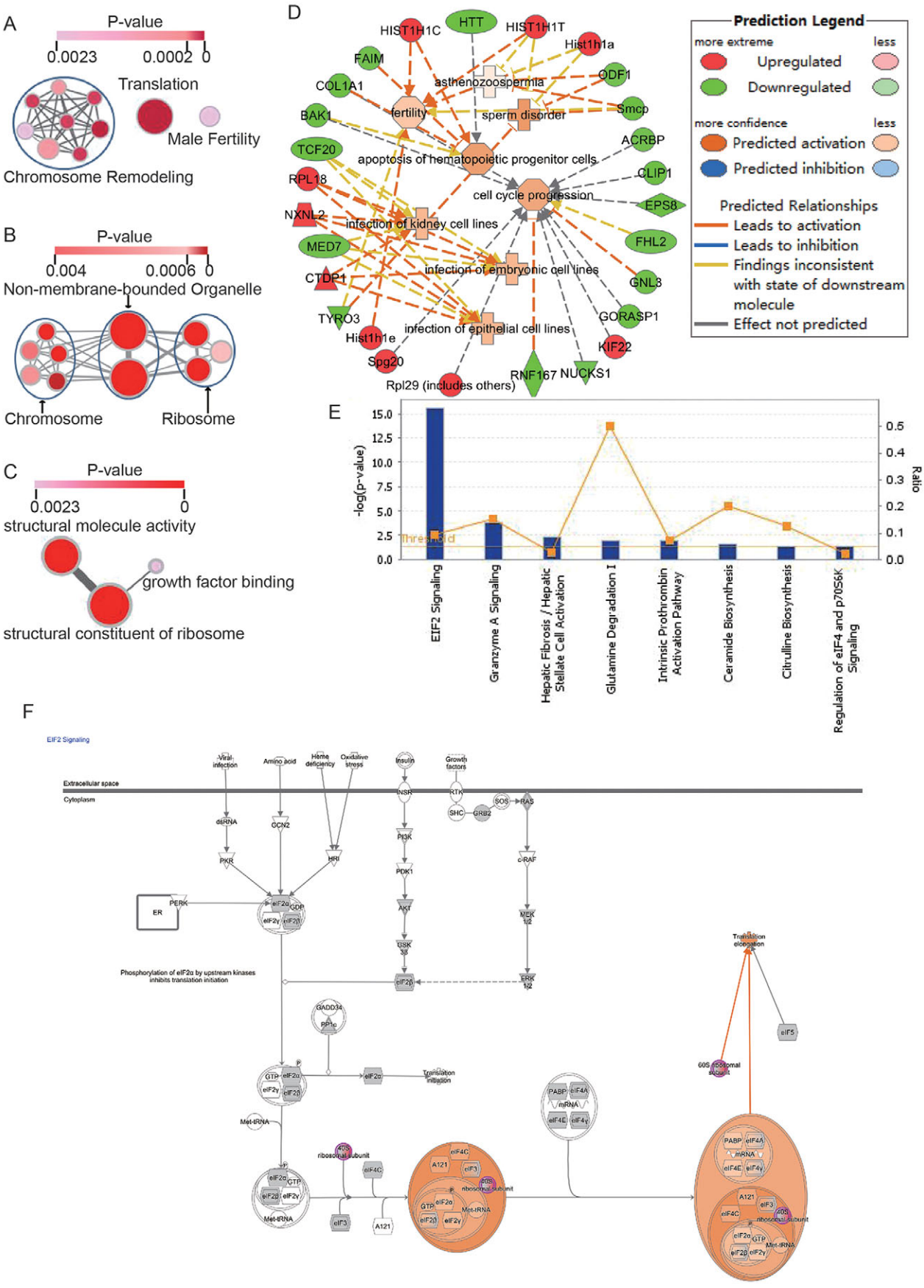

Fig. 7. See next page for legend.

Journal of Cell Science

Journal of Cell Science (2016) 129, 492-501 doi:10.1242/jcs.173666

Fig. 7. Functional annotations of proteins involving spermiogenesis impairment induced by knockout of *Htt* reveal an enrichment for translation and DNA packaging proteins. (A–C) Overview of GO Slim generic distribution of differentially expressed proteins in mouse testis induced by knockout of *Htt* using Enrichment (version 2.44), a plugin of Cytoscape. (A) Biological process analysis; (B) cellular component analysis; (C) molecular function analysis. Each annotation is color-coded according to its corrected *P*-value (see color bar), which indicates the degree of overrepresentation in data compared to the complete *Mus musculus* proteome. (D) Diseases and disorder analyses of differentially expressed proteins in IPA. (E) The most significant canonical pathways in which the differentially expressed genes were enriched. 119 differentially expressed genes were applied to the Ingenuity pathway analysis (IPA) software, and the most significant canonical pathways are shown. (F) Eif2 signaling was predicted to be activated in *Htt*-deficient testis by IPA. The prediction was based on the expression of associated proteins in comparison of proteomics data. The red 40S and 60S were detected to be activated in *Htt*-deficient testes. Then the Molecule Activity Predictor (MAP) propagated the effects to neighboring molecules. The blue color indicates predicted inhibition (or decreased activity), and the orange color represents predicted activation (or increased activity). The intensity of color indicates the confidence of the prediction. If confidence is high, nodes will be darker orange or blue; as confidence decreases, the shade of orange and blue become paler. The arrowheads indicate the expected effect from the literature, and the edge color signifies the effect the upstream molecule has on the downstream molecule, given the activity of those molecules. The prediction legend of F is the same as in D. Results are $P<0.005$, with an FDR $q<0.1$ and a overlap cutoff >0.5.

Functional annotation of differentially expressed proteins in the absence of *Htt*

We used the web tool provided by the DAVID website (http://david.abcc.ncifcrf.gov/) to search for functional annotation terms (FATs) that are enriched in the above differentially expressed proteins (DEPs) (Table S2; Fig. 7A–C). Gene Ontology (GO) categories were ranked by their corrected *P*-value, which indicates the degree of overrepresentation in the significantly DEPs compared with the complete *Mus musculus* proteome. We found that the DEPs were enriched in biological processes such as 'translation' and 'DNA packaging', as well as male fertility (Table S2; Fig. 7A). A large number of proteins involved in translation were differentially expressed upon Htt inactivation, including 18 ribosomal proteins (RL28, RS16, RS8, RL36A, RS9, RL24, RL4, RL27, RL13, RL34, RL26, RL7, RL15, RL18A, RL29, RL18, RL6 and RL14) and a tRNA ligase protein (SYAM, also known as AARS2). Consistently, 'ribosome' and 'structural constituent of ribosome' were the most significantly enriched cellular components and molecular functions, respectively (Table S2; Fig. 7B,C). Additionally, Htt deficiency activated the expression of six histone proteins (H11, H4, H1T, H15, H14 and H12), whereas it repressed the other four proteins (EP400, SMC2, PRM3 and KDM3B) related to DNA packaging (Table S2). In line with the enrichment of 'Chromosome remodeling' in the biological process, the cellular component term 'Chromosome' was also significantly enriched (Table S2; Fig. 7B).

To understand how Htt deletion affects spermatogenesis, we performed comprehensive bioinformatic analysis using Ingenuity pathway analysis (IPA) to assess integrated function and pathways of these DEPs. The most significant functions and diseases related to these proteins analyzed in IPA belonged to a network consisting of 27 proteins involved in sperm disorder, apoptosis of hematopoietic progenitor cells, cell cycle progression, the infection of kidney cell lines, the infection of epithelial cell lines, the infection of embryonic cell lines, fertility and azoospermia (Fig. 7D). In particular, the markedly down-expressed proteins upon Htt depletion, such as ODF1, Smcp, ACRBP, CLIP1, EPS8, TYRO3 and BAK1, have been reported to be directly linked to spermatogenesis and male fertility (Baba et al., 1994; Oldereid et al., 2001; Nayernia et al., 2002; Akhmanova et al., 2005; Xiong et al., 2008; Cheng et al., 2011; Yang et al., 2012). Thus, knockout of Htt might impair spermatogenesis through altering the expression of these proteins. We also annotated the mouse phenotype related to male reproduction of DEPs from the Mouse Genome Informatics (MGI) database (Table S3) (Blake et al., 2014). We next investigated post-transcriptional regulation of gene expression in *Htt* CKO testes by comparing changes at protein levels with changes at transcript levels of these 27 DEPs (Fig. S2A,B). We found that the mRNA levels of eight downregulated proteins in *Htt* CKO were significantly lower than those of their counterparts in WT controls and the mRNA levels of six downregulated proteins in *Htt* CKO were not significantly changed (Fig. S2A). Among the 11 upregulated proteins, the mRNA levels of two proteins were significantly lower in *Htt* CKO than in control, whereas the mRNA levels of eight proteins did not change significantly (Fig. S2B). To further verify our iTRAQ data, we selected two up-regulated proteins for western blot analysis. As shown in Fig. S2C, the expression of SPG20 and RPL29 proteins was significantly upregulated in Htt CKO testes compared to the controls (Fig. S2C).

IPA results showed that the 119 DEPs were mainly enriched in Eif2 signaling and Granzyme A signaling pathways (Fig. 7E), which are related to translation and DNA packaging, respectively. Based on the analysis of DEPs with the Molecule activity predictor (MAP) in IPA, the elongation of translation was predicted to be hyperactivated in Htt-knockout testis (Fig. 7F). Eukaryotic translation initiation factor 2 (Eif2) signaling was predicted to be activated based on the upregulation of 17 ribosomal proteins. This translation activation is likely induced by knockout of *Htt*, as WT Htt functions with Ago2, the catalytic component of the RNA-induced-silencing complex, in a post-transcriptional gene silencing pathway, and its overexpression strongly inhibited translation in HeLa cell extracts (Savas et al., 2008; Culver et al., 2012).

Taken together, the protein expression profiles between control and *Htt* CKO testes were compared and those differentially expressed genes were applied to DAVID and IPA. The enrichment of gene clusters related to translation and chromosome remodeling was identified. IPA results show that translation is predicted to be hyperactivated in *Htt* CKO testis, which is consistent with previous studies (Savas et al., 2008; Culver et al., 2012). Hence, there might be a link between the abnormal translation and male infertility in absence of Htt.

DISCUSSION

Although a number of genes are known to be involved in spermatogenesis, only a few possess clean-cut arrest phenotypes indicative of their role in the global regulation of key spermatogenic steps. In this study, we have presented, for the first time, evidence that *Htt* is such a spermatogenic gene. Here, the phenotype of male sterility, azoospermia and spermiogenesis arrest in *Htt* CKO mouse reveals the essential role of Htt in spermiogenesis.

A previous work from Scott Zeitlin's group had detected a reduction of Htt expression in testis and male fertility following Cre-mediated recombination using a Camk2a-cre transgene (Dragatsis et al., 2000). Given that the Camk2a-cre lines they used can induce a simultaneous deletion of floxed *Htt* gene in the brain and male germ cells (Choi et al., 2014), the possibility that the sterility they observed could be due to an impaired hypothalamic–pituitary–testis axis caused by the Cre-mediated recombination in the brain could not be excluded. In this study, we generated a CKO mouse that had conditional knockout of *Htt* specifically in the male germ cells. The *Htt* CKO mouse showed complete sterility, loss of germ cells and

Journal of Cell Science (2016) 129, 492-501 doi:10.1242/jcs.173666

spermatogenesis arrest at the early spermatid stage in seminiferous tubules. These results indicate that Htt has a crucial function in spermatogenesis. It is known that Huntington's disease patients and animal models have specific testicular pathology with reduced numbers of germ cells and abnormal seminiferous tubule morphology (Van Raamsdonk et al., 2007). We speculate that the testicular degeneration in Huntington's disease patients and mouse models might be attributable to the partial loss of normal Htt function.

To further elucidate the molecular mechanisms underlying spermatogenesis defects in *Htt*-deleted testes, we undertook a comparative proteomics analysis and discovered 119 differentially expressed proteins (Table S4). Eleven upregulated proteins and 16 downregulated proteins have been previously shown to be essential for spermatogenesis (Fig. 7D). The knockout of *Htt* might impair spermatogenesis through disturbing the expression of these spermatogenesis regulators. In addition, some other differentially expressed proteins might also contribute to the *Htt*-deletion-induced male fertility.

Htt localizes in P granules and is involved in RNA storage in germ cells (Culver et al., 2012). It also associates with Ago2, the catalytic component of the RNA-induced silencing complex, with involvement in RNA transport in cultured cortical neurons (Savas et al., 2008, 2010). Recently, both WT and mHtt have been found to co-purify with several translation-related proteins and co-fractionate with ribosomes (Culver et al., 2012). Furthermore, the overexpression of Htt inhibits cap-dependent translation of a reporter mRNA in an *in vitro* system (Culver et al., 2012). During spermiogenesis, translational control is essential because *de novo* protein production is needed for the terminal steps of germ cell differentiation, which occur after transcription has ended. In our study, Gene Ontology analysis of those *Htt* deletion-induced DEPs revealed a statistically significant enrichment for proteins involved in translation, among multiple categories (Fig. 7). The elongation of translation was predicted to be hyperactivated in *Htt*-knockout testis through further analysis of DEPs in IPA (Fig. 7F). Thus, we speculate that Htt might function as a regulator of post-transcription required for spermiogenesis. This possibility is suggested not only from the translation association but also from the existence of three RNA-binding proteins, RBM28, RBMX2 and RBM19, and three E3 ligases, RNF167, LTN1, MYCB2 involved in proteosome degradation identified among our differentially expressed proteins (Table S3). This proteomic analysis will be a valuable resource to help characterize important proteins involved in spermatogenesis and in revealing their mechanisms of action.

In addition to arrest at the round spermatid stage, some tubules of 6-week-old *Htt* CKO mice show more than one layer of zygotene or pachytene spermatocytes (Fig. 3C–F). Given that no other appreciable meiotic defects could be detected in *Htt* CKO mice, we speculate that this abnormality might be an indirect effect of prolonged spermiogenetic arrest. In support of this interpretation, TUNEL analysis showed a striking increase of apoptotic germ cells in *Htt* CKO mice, limited to round spermatids. Similar to nonspecific defects, apoptosis, for example, is frequently seen in spermatid-arrested mutants (Martianov et al., 2001; Zhang et al., 2001; Deng and Lin, 2002).

In our study, knockout of *Htt* in male germ cells results in infertility and spermatogenesis arrest at the round spermatid stage. A range of proteins regulated by Htt was identified through comparative proteomics. These Htt-regulated proteins are involved in translation and DNA packaging. Thus, Htt could be important for regulating the translation of crucial genes and DNA packaging at specific times during spermatogensis. Mice deficient in Htt expression protein could serve as a model system for the study of male reproduction and fertility control. A better understanding of mouse Htt will shed light on the role of HTT in human infertility and Huntington's disease.

MATERIALS AND METHODS

Mice

Mice harboring two conditional *Htt* alleles ($Htt^{flox/flox}$) were generated as described previously, in which LoxP sequences were inserted 1.3 kb upstream of the *Htt* transcription initiation site and within intron 1 (Dragatsis et al., 2000). The Stra8-cre transgenic mice were purchased from the Jackson Laboratory. The breeding of the $Htt^{flox/flox}$ with Stra8-cre mice to generate the *Htt* CKO mice was as described in Fig. 1A. Specifically, to achieve specific deletion of *Htt* gene in germ cells, the female mice, which were homozygous for *Htt* flox alleles, were crossed with male Stra8-cre mice. The heterozygous progenies, with the genotype of $Htt^{flox/+}$/Stra8-cre were inbred to obtain the female $Htt^{flox/\Delta}$Stra8-cre mice, which were further crossed with male $Htt^{flox/flox}$ mice to produce male $Htt^{flox/\Delta}$/Stra8-cre mice, $Htt^{flox/flox}$/Stra8-cre mice, $Htt^{flox/\Delta}$ mice and $Htt^{flox/flox}$ mice. The male $Htt^{flox/\Delta}$/Stra8-cre mice and $Htt^{flox/flox}$/Stra8-cre mice were used as CKO groups, whereas the male $Htt^{flox/\Delta}$ mice and $Htt^{flox/flox}$ mice were used as control groups. The PCR genotyping primers for WT, floxed and Cre alleles of *Htt* are listed below: for the WT allele, forward 5′-CGGGCTTATACCCCTACAGT-3′ and reverse 5′-AAGCCAAGCAGTGATAGAACACA-3′; for the floxed allele, forward 5′-CTAAAGCGCATGCTCCAGACTG-3′ and reverse 5′-AGATCTCTGAGTTATAGGTCAGC-3′; for the delta allele (Δ), forward 5′-CTAAAGCGCATGCTCCAGACTG-3′ and reverse 5′-CTGGCTGGC-CTGACCCGGCT-3′; and for the Cre allele, forward 5′-GTGCAAGCTG-AACAACAGGA-3′ and reverse 5-AGGGACACAGCATTGGAGTC. All the mice were maintained on a C57BL/6; 129/SvEv mixed genetic background. The mice were housed in cages under a 12-h-light–12-h-dark cycle. All the animal procedures were reviewed and approved by the Institute of Zoology, Institutional Animal Care and Use Committee, and were conducted according to the committee's guidelines.

Fertility and epididymal sperm counts

For fertility testing, 8-week-old *Htt* CKO and control male mice were singly housed with wild-type 129 females. Copulatory plugs were monitored daily, and plugged females were moved to separate cages for monitoring pregnancy. Females that were not pregnant within 2 weeks were replaced. The mating process lasted for 3 months. Viable pups were counted on the first day of life.

Caudal epididymides from each 8-week-old mouse were minced with fine forceps in a petri dish with 37°C phosphate-buffered saline (PBS), and assessed under a microscope. Sperm were counted with a haemocytometer under a light microscope after being fixed in 10% neutral-buffered formalin.

Histology, immunostaining and TUNEL

Testis cell preparations were generated from 3-, 6- or 8-week-old mice. Usually, one testis was used for immunohistochemistry and the other was processed for surface spreading according to established protocol (Moens et al., 2000). For histology, testes were fixed with Bouin's fixatives (Polysciences) overnight at 4°C, dehydrated in an ethanol series and embedded in paraffin wax. Paraffin sections (5 µm) were cut and then stained with hematoxylin-eosin or periodic acid schiff (PAS)–hematoxylin to visualize the acrosome. Stages of seminiferous epithelium cycle and steps of spermatid development were determined as described previously (Ahmed and de Rooij, 2009). For immunostaining, paraffin-embedded sections of testis were used for staining Plzf (Millipore, 100105, 1:400), PCNA (Santa Cruz Biotechnology, sc-7907, 1:800), Dazl (AbD Serotec, MCA2336, 1:1000), γH2AX (Millipore, 16-193, 1:1000), Protamine 2 (Prm2) (Santa Cruz Biotechnology, sc23104, 1:200), RPL29 (Proteintech, 15799-1-AP, 1:400) and SPG20 (Proteintech, 13791-1-AP, 1:500). After deparaffinization and rehydration, slides were incubated with boiling 0.01 M sodium citrate (pH 6.0) for 10 min to retrieve the antigens before immunostaining. Standard immunostaining procedures were used. For detection of apoptotic cells (TUNEL assays), slides were fixed in 4% (w/v) paraformaldehyde (PFA) in PBS for 15 min at room temperature after deparaffinization and rehydration. TUNEL-positive cells were detected using the In Situ Cell Death Detection

Kit, Fluorescein (Roche, Switzerland), and the sections were counterstained with 0.1% (w/v) 4,6-diamidino-2-phenylindoledihydro-chloride (DAPI) from Sigma-Aldrich. The images were taken using a Nikon TiE microscope and a confocal laser microscope (LSM510, Carl Zeiss, Oberkochen, Germany) with an argon ion laser.

Germ cell nuclear spreads preparations and immunofluorescent staining

Nuclear spreads destined for immunostaining were obtained from testes at 6 weeks of age to enrich for meiosis stages and were carried out as described previously (Peters et al., 1997; Cai et al., 2011). Slides were incubated with indicated primary antibodies diluted in PBST (PBS containing 10% goat serum, 3% bovine serum albumin and 0.05% Triton X-100) for ∼24 h at 37°C in a humidified chamber. Then, slides were incubated with the appropriate secondary antibodies for 90 min at 37°C in the dark. Images were taken with a Leica fluorescence microscope. The primary antibodies include mouse γH2AX (Millipore, 16-193, 1:1000), rabbit SYCP1 (abcam, ab15090, 1:200), rabbit SYCP3 (abcam, ab15093, 1:200), goat SYCP3 (abcam, sc-20845, 1:200), mouse MLH1 (BD Pharmingen, 551091, 1:50), human CREST (Immunovision, HSM0101, 1:800). The secondary antibodies were Alexa-Fluor-488-labeled donkey anti-mouse-IgG, Alexa-Fluor-488-labeled donkey anti-rabbit-IgG, Alexa-Fluor-568-labeled donkey anti-goat-IgG (Molecular Probes, Eugene, OR) and Dylight 405-labeled donkey anti-human-IgG (Abbkine, CA) antibodies. The stages of prophase I meiosis were categorized based on the distribution of the synaptonemal complex proteins SYCP3 and SYCP1 together with the kinetics of CREST. The experiment was repeated at least three times. The immunofluorescence images were taken with a Nikon/Perkin-Elmer spinning disc confocal microscopy system.

Tissue lysis, protein extraction, protein digestion and iTRAQ labeling

Testes from *Htt* CKO mice and the controls (n=6) at 5 weeks of age were harvested and fast frozen in liquid nitrogen. Samples were ground and precipitated with pre-chilled trichloroacetic acid (TGA) and acetone for several times until they turned white. The prepared testis tissues were dissolved in the lysis buffer (8 M urea, 30 mM HEPES, 1 mM PMSF, 2 mM EDTA, 10 mM DTT) and sonicated. The homogenate was centrifuged at 20,000 ***g*** for 30 min. For the iTRAQ experiments, the testis proteins were reduced with 10 mM DTT at 56°C for 1 h, and alkylated with 55 mM iodoacetamide (IAM) at room temperature for 1 h in the dark. The treated proteins were precipitated in acetone at −20°C for 3 h. After centrifugation at 20,000 ***g*** for 30 min, the protein pellet was resuspended and ultrasonicated in pre-chilled 200 mM triethylammonium bicarbonate (TEAB, Sigma, 15715-58-9) buffer with 0.1% SDS for 3 min. The proteins were finally harvested after centrifugation at 20,000 ***g*** for 30 min. Equal amounts of proteins from each testis in each group were mixed and grouped into two pools. Then the digestion was performed by adding sequencing-grade trypsin (Promega, Madison, WI) at 37°C overnight. The tryptic peptides were desalted and labeled with iTRAQ 4 plex reagents (Applied Biosystem) according to the manufacturer's protocol. The testis peptides from control groups and knockout groups were labeled with iTRAQ reagent 113, 114, 118 and 119, respectively.

Two-dimensional chromatography to separate the iTRAQ-labeled peptides followed by identification through mass spectrometry

The labeled peptides were pooled and dried by vacuum centrifugation. SCX chromatography was performed with a Shimadzu HPLC system connected to a Phenomenex Luna SCX column (25 cm×4.6 mm, 5 mm, 100A). Equal amounts of the iTRAQ-labeled peptides from all four samples were mixed, the pH of the peptide mixture was adjusted to 3 and the mixture was loaded onto the SCX column which was equilibrated with buffer A (10 mM KH_2PO_4 and 25% acetonitrile, pH 3.0). Then, the peptide mixture was eluted with buffer A for 10 min, and a gradient program with the elution buffer B (10 mM KH_2PO_4, 25% acetonitrile and 2 M KCl, pH 3): 0–5% within 36 min, 5–30% within 56 min, 30–50% within 61 min, 50–60% within 66 min and 50–100% within 81 min. The flow rate of the high-pressure liquid chromatography (HPLC) was 1 ml/min. The peptide elution was monitored at 214 nm. A total of 30 eluted fractions were collected and desalted with a Strata X C18 column (Phenomenex), and vacuum-dried. Triple time-of-flight (TOF) MS/MS (Q Enactive, Thermo Fisher Scientific, USA) with a NanoLC system was used for peptide identification.

RNA extraction and real-time PCR

Testes were harvested in TRIzol reagent (1 ml reagent per 50–100 mg testis; Invitrogen). RNA was extracted according to the manufacturer's instructions and quantified by measurement of the optical density at 260 nm. Reverse transcription was carried out following standard procedures using random primers and Quant Reverse Transcriptase (TIANGEN, China). Real-time PCR was performed with an ABI Prism 7000 device (Applied) using UltraSYBR Mixture (CWBIO, China) and the primers given in Table S4. Three samples from different mice for each group were used. Quantifications were made in triplicate for each sample from individual testes. For analysis of the mRNA expression, the comparative Ct method (ΔΔCT) with *Gapdh* mRNA as the internal control was used (Livak and Schmittgen, 2001).

Data processing

The data files of each fraction were combined together to perform searching against *Mus musculus* protein database (uniprot2014_mus) using PD software (Protein Discoverer 1.3, Thermo). The searching parameters were set as, one missed cleavage, carbamidomethylation of cystein as fixed modification, oxidation of methionine, N-terminal iTRAQ 8 plex mass addition lysine and iTRAQ 8 plex mass addition on tyrosine, and N-terminal pyroglutamylation as variable modifications. Mascot software (version 2.3.0, http://www.Matrixscience.com/search_form_select.html) was employed to calculate the iTRAQ quantification with the Mascot files. In order to achieve a high-quality mass spectrometry signal for quantification, the peptides served as the quantitative evaluation were selected as meeting: (1) a target FDR threshold set ≤1% at the peptide level, (2) a minimum required peptide length of six amino acids, and (3) proteins that contain at least one tag-labeled unique peptide.

Gene Ontology (GO) annotation of the identified proteins was performed by searching the DAVID website (http://david.abcc.ncifcrf.gov/). GO terms enrichment analysis of the differentially expressed proteins was performed with Cytoscape and its plugin EnrichmentMap (version 2.0.1), which is a java-based tool used to visualize the results of gene-set enrichment as a network. To better understand these differentially expressed proteins in relation to published literature, interactions among these proteins regarding function and disease, and biological pathway were determined using IPA (www.ingenuity.com). Uniprot accession was used as the identifier and the Ingenuity knowledge gene database was used as a reference for the pathway analysis.

Statistical analysis

Chi-squared analysis was carried out to test differences in meiotic stage distribution in mutant and WT spermatocytes. A nonparametric or independent sample t-test was used to determine significant differences of testis weight, the number of MLH1 foci per spermatocyte and the number of apoptotic cells per tubule between the control and CKO groups. For all tests, statistical significance was taken as $P \leq 0.05$. At least three mice per genotype were used for each experiment.

Acknowledgements

The authors thank Drs Jiahao Sha, Yixun Liu, Chunsheng Han, Fei Gao, Scott O. Zeitlin, Ioannis Dragatsis for reagents or mice, Dr Qinghua Shi for instructions on chromatin spread preparation, and Drs Xiaomin Lou, Ju Zhang, Hongyan Shen for help with iTRAQ assay.

Competing interests

The authors declare no competing or financial interests.

Author contributions

C.G. and T.-S.T. conceived the study and designed experiments; J.Y., H.Z., Y.L., F.Z., S.Z. and C.X. performed experiments. J.Y., T.-S.T. and C.G. analyzed the data and wrote the manuscript. All authors read and approved the manuscript for publication.

Funding
This work was supported by the Chinese National 973 Project [grant numbers 2012CB944702, 2013CB945003, 2011CB944302]; the National Natural Science Foundation of China [grant numbers 31471331, 31170730, 31570816, 91519324, 81371415, 31301228, 31100557, 31300658, 31470784, 81300982]; the Strategic Priority Research Program of the CAS [grant number XDB14030302]; and the Chinese Academy of Sciences/State Administration of Foreign Experts Affairs International Partnership Program for Creative Research Teams; and the State Key Laboratory of Membrane Biology.

Supplementary information
Supplementary information available online at
http://jcs.biologists.org/lookup/suppl/doi:10.1242/jcs.173666/-/DC1

References

Ahmed, E. A. and de Rooij, D. G. (2009). Staging of mouse seminiferous tubule cross-sections. *Methods Mol. Biol.* **558**, 263-277.
Akhmanova, A., Mausset-Bonnefont, A.-L., van Cappellen, W., Keijzer, N., Hoogenraad, C. C., Stepanova, T., Drabek, K., van der Wees, J., Mommaas, M., Onderwater, J. et al. (2005). The microtubule plus-end-tracking protein CLIP-170 associates with the spermatid manchette and is essential for spermatogenesis. *Genes Dev.* **19**, 2501-2515.
Auerbach, W., Hurlbert, M. S., Hilditch-Maguire, P., Wadghiri, Y. Z., Wheeler, V. C., Cohen, S. I., Joyner, A. L., MacDonald, M. E. and Turnbull, D. H. (2001). The HD mutation causes progressive lethal neurological disease in mice expressing reduced levels of huntingtin. *Hum. Mol. Genet.* **10**, 2515-2523.
Baba, T., Niida, Y., Michikawa, Y., Kashiwabara, S., Kodaira, K., Takenaka, M., Kohno, N., Gerton, G. L. and Arai, Y. (1994). An acrosomal protein, sp32, in mammalian sperm is a binding protein specific for two proacrosins and an acrosin intermediate. *J. Biol. Chem.* **269**, 10133-10140.
Blake, J. A., Bult, C. J., Eppig, J. T., Kadin, J. A., Richardson, J. E. and **The Mouse Genome Database Group**. (2014). The Mouse Genome Database: integration of and access to knowledge about the laboratory mouse. *Nucleic Acids Res.* **42**, D810-D817.
Cai, X., Li, J., Yang, Q. and Shi, Q. (2011). Gamma-irradiation increased meiotic crossovers in mouse spermatocytes. *Mutagenesis* **26**, 721-727.
Cattaneo, E., Zuccato, C. and Tartari, M. (2005). Normal huntingtin function: an alternative approach to Huntington's disease. *Nat. Rev. Neurosci.* **6**, 919-930.
Cheng, C. Y., Lie, P. P. Y., Wong, E. W. P., Mruk, D. D. and Silvestrini, B. (2011). Adjudin disrupts spermatogenesis via the action of some unlikely partners: Eps8, Arp2/3 complex, drebrin E, PAR6 and 14-3-3. *Spermatogenesis* **1**, 291-297.
Choi, C.-I., Yoon, S.-P., Choi, J.-M., Kim, S.-S., Lee, Y.-D., Birnbaumer, L. and Suh-Kim, H. (2014). Simultaneous deletion of floxed genes mediated by CaMKIIalpha-Cre in the brain and in male germ cells: application to conditional and conventional disruption of Goalpha. *Exp. Mol. Med.* **46**, e93.
Costoya, J. A., Hobbs, R. M., Barna, M., Cattoretti, G., Manova, K., Sukhwani, M., Orwig, K. E., Wolgemuth, D. J. and Pandolfi, P. P. (2004). Essential role of Plzf in maintenance of spermatogonial stem cells. *Nat. Genet.* **36**, 653-659.
Culver, B. P., Savas, J. N., Park, S. K., Choi, J. H., Zheng, S., Zeitlin, S. O., Yates, J. R., III and Tanese, N. (2012). Proteomic analysis of wild-type and mutant huntingtin-associated proteins in mouse brains identifies unique interactions and involvement in protein synthesis. *J. Biol. Chem.* **287**, 21599-21614.
Deng, W. and Lin, H. (2002). miwi, a murine homolog of piwi, encodes a cytoplasmic protein essential for spermatogenesis. *Dev. Cell* **2**, 819-830.
Dragatsis, I., Levine, M. S. and Zeitlin, S. (2000). Inactivation of Hdh in the brain and testis results in progressive neurodegeneration and sterility in mice. *Nat. Genet.* **26**, 300-306.
Gil, J. M. and Rego, A. C. (2008). Mechanisms of neurodegeneration in Huntington's disease. *Eur. J. Neurosci.* **27**, 2803-2820.
Hamer, G., Roepers-Gajadien, H. L., van Duyn-Goedhart, A., Gademan, I. S., Kal, H. B., van Buul, P. P. W. and de Rooij, D. G. (2003). DNA double-strand breaks and gamma-H2AX signaling in the testis. *Biol. Reprod.* **68**, 628-634.
Idler, R. K. and Yan, W. (2012). Control of messenger RNA fate by RNA-binding proteins: an emphasis on mammalian spermatogenesis. *J. Androl.* **33**, 309-337.
Karp, N. A., Huber, W., Sadowski, P. G., Charles, P. D., Hester, S. V. and Lilley, K. S. (2010). Addressing accuracy and precision issues in iTRAQ quantitation. *Mol. Cell. Proteomics* **9**, 1885-1897.
Kleene, K. C. (2013). Connecting cis-elements and trans-factors with mechanisms of developmental regulation of mRNA translation in meiotic and haploid mammalian spermatogenic cells. *Reproduction* **146**, R1-R19.
Leavitt, B. R., Guttman, J. A., Hodgson, J. G., Kimel, G. H., Singaraja, R., Vogl, A. W. and Hayden, M. R. (2001). Wild-type huntingtin reduces the cellular toxicity of mutant huntingtin in vivo. *Am. J. Hum. Genet.* **68**, 313-324.
Li, Y.-C., Hu, X.-Q., Zhang, K.-Y., Guo, J., Hu, Z.-Y., Tao, S.-X., Xiao, L.-J., Wang, Q.-Z., Han, C.-S. and Liu, Y.-X. (2006). Afaf, a novel vesicle membrane protein, is related to acrosome formation in murine testis. *FEBS Lett.* **580**, 4266-4273.
Lifschitz-Mercer, B., Elliott, D. J., Issakov, J., Leider-Trejo, L., Schreiber, L., Misonzhnik, F., Eisenthal, A. and Maymon, B. (2002). Localization of a specific germ cell marker, DAZL1, in testicular germ cell neoplasias. *Virchows Archiv* **440**, 387-391.
Livak, K. J. and Schmittgen, T. D. (2001). Analysis of relative gene expression data using real-time quantitative PCR and the 2(-Delta Delta C(T)) Method. *Methods* **25**, 402-408.
Martianov, I., Fimia, G.-M., Dierich, A., Parvinen, M., Sassone-Corsi, P. and Davidson, I. (2001). Late arrest of spermiogenesis and germ cell apoptosis in mice lacking the TBP-like TLF/TRF2 gene. *Mol. Cell* **7**, 509-515.
Moens, P. B., Freire, R., Tarsounas, M., Spyropoulos, B. and Jackson, S. P. (2000). Expression and nuclear localization of BLM, a chromosome stability protein mutated in Bloom's syndrome, suggest a role in recombination during meiotic prophase. *J. Cell Sci.* **113**, 663-672.
Nantel, F., Monaco, L., Foulkes, N. S., Masquilier, D., LeMeur, M., Henriksen, K., Dierich, A., Parvinen, M. and Sassone-Corsi, P. (1996). Spermiogenesis deficiency and germ-cell apoptosis in CREM-mutant mice. *Nature* **380**, 159-162.
Nasir, J., Floresco, S. B., O'Kusky, J. R., Diewert, V. M., Richman, J. M., Zeisler, J., Borowski, A., Marth, J. D., Phillips, A. G. and Hayden, M. R. (1995). Targeted disruption of the Huntington's disease gene results in embryonic lethality and behavioral and morphological changes in heterozygotes. *Cell* **81**, 811-823.
Nayernia, K., Adham, I. M., Burkhardt-Gottges, E., Neesen, J., Rieche, M., Wolf, S., Sancken, U., Kleene, K. and Engel, W. (2002). Asthenozoospermia in mice with targeted deletion of the sperm mitochondrion-associated cysteine-rich protein (Smcp) gene. *Mol. Cell. Biol.* **22**, 3046-3052.
Nguyen-Chi, M. and Morello, D. (2011). RNA-binding proteins, RNA granules, and gametes: is unity strength? *Reproduction* **142**, 803-817.
Oakberg, E. F. (1956). A description of spermiogenesis in the mouse and its use in analysis of the cycle of the seminiferous epithelium and germ cell renewal. *Am. J. Anat.* **99**, 391-413.
Oldereid, N. B., Angelis, P. D., Wiger, R. and Clausen, O. P. F. (2001). Expression of Bcl-2 family proteins and spontaneous apoptosis in normal human testis. *Mol. Hum. Reprod.* **7**, 403-408.
Paronetto, M. P. and Sette, C. (2010). Role of RNA-binding proteins in mammalian spermatogenesis. *Int. J. Androl.* **33**, 2-12.
Peters, A. H. F. M., Plug, A. W., van Vugt, M. J. and de Boer, P. (1997). A drying-down technique for the spreading of mammalian meiocytes from the male and female germline. *Chromosome Res.* **5**, 66-68.
Russell, L. D., Ettlin, R. A., Hikim, A. P. S. and Clegg, E. D. (1990). *Histological and Histopathological Evaluation of the Testis*, pp. 120-161. Florida: Cache River Press.
Savas, J. N., Makusky, A., Ottosen, S., Baillat, D., Then, F., Krainc, D., Shiekhattar, R., Markey, S. P. and Tanese, N. (2008). Huntington's disease protein contributes to RNA-mediated gene silencing through association with Argonaute and P bodies. *Proc. Natl. Acad. Sci. USA* **105**, 10820-10825.
Savas, J. N., Ma, B., Deinhardt, K., Culver, B. P., Restituito, S., Wu, L., Belasco, J. G., Chao, M. V. and Tanese, N. (2010). A role for Huntington disease protein in dendritic RNA granules. *J. Biol. Chem.* **285**, 13142-13153.
Van Raamsdonk, J. M., Murphy, Z., Selva, D. M., Hamidizadeh, R., Pearson, J., Petersen, A., Bjorkqvist, M., Muir, C., Mackenzie, I. R., Hammond, G. L. et al. (2007). Testicular degeneration in Huntington disease. *Neurobiol. Dis.* **26**, 512-520.
Vernet, N., Dennefeld, C., Guillou, F., Chambon, P., Ghyselinck, N. B. and Mark, M. (2006). Prepubertal testis development relies on retinoic acid but not rexinoid receptors in Sertoli cells. *EMBO J.* **25**, 5816-5825.
White, J. K., Auerbach, W., Duyao, M. P., Vonsattel, J.-P., Gusella, J. F., Joyner, A. L. and MacDonald, M. E. (1997). Huntingtin is required for neurogenesis and is not impaired by the Huntington's disease CAG expansion. *Nat. Genet.* **17**, 404-410.
Xiong, W., Chen, Y., Wang, H., Wang, H., Wu, H., Lu, Q. and Han, D. (2008). Gas6 and the Tyro 3 receptor tyrosine kinase subfamily regulate the phagocytic function of Sertoli cells. *Reproduction* **135**, 77-87.
Yang, K., Meinhardt, A., Zhang, B., Grzmil, P., Adham, I. M. and Hoyer-Fender, S. (2012). The small heat shock protein ODF1/HSPB10 is essential for tight linkage of sperm head to tail and male fertility in mice. *Mol. Cell. Biol.* **32**, 216-225.
Zeitlin, S., Liu, J.-P., Chapman, D. L., Papaioannou, V. E. and Efstratiadis, A. (1995). Increased apoptosis and early embryonic lethality in mice nullizygous for the Huntington's disease gene homologue. *Nat. Genet.* **11**, 155-163.
Zhang, D., Penttila, T.-L., Morris, P. L., Teichmann, M. and Roeder, R. G. (2001). Spermiogenesis deficiency in mice lacking the Trf2 gene. *Science* **292**, 1153-1155.
Zhang, H., Lu, Y., Luo, B., Yan, S., Guo, X. and Dai, J. (2014). Proteomic analysis of mouse testis reveals perfluorooctanoic acid-induced reproductive dysfunction via direct disturbance of testicular steroidogenic machinery. *J. Proteome Res.* **13**, 3370-3385.